

THE LINK BETWEEN LIGHT AND MASS IN LATE-TYPE SPIRAL GALAXY DISKS

ROBERT A. SWATERS¹, MATTHEW A. BERSHADY², THOMAS P. K. MARTINSSON³,KYLE B. WESTFALL⁴, DAVID R. ANDERSEN⁵, AND MARC A. W. VERHEIJEN⁶¹ National Optical Astronomical Observatory, 950 North Cherry Avenue, Tucson, AZ 85719, USA; rob@swaters.net² Department of Astronomy, University of Wisconsin, 475 North Charter Street, Madison, WI 53706, USA³ Leiden Observatory, Leiden University, P.O. Box 9513, 2300 RA Leiden, The Netherlands⁴ Institute of Cosmology and Gravitation, University of Portsmouth, Dennis Sciama Building, Burnaby Road, Portsmouth PO1 3FX, UK⁵ NRC Herzberg Programs in Astronomy and Astrophysics, 5071 West Saanich Road, Victoria, BC, V9E 2E7, Canada⁶ University of Groningen, Kapteyn Astronomical Institute, Landleven 12, 9747-AD Groningen, The Netherlands

Received 2014 September 15; accepted 2014 November 10; published 2014 December 9

ABSTRACT

We present the correlation between the extrapolated central disk surface brightness (μ) and extrapolated central surface mass density (Σ) for galaxies in the DiskMass sample. This μ – Σ relation has a small scatter of 30% at the high surface brightness (HSB) end. At the low surface brightness (LSB) end, galaxies fall above the μ – Σ relation, which we attribute to their higher dark matter content. After correcting for the dark matter as well as for the contribution of gas and the effects of radial gradients in the disk, the LSB end falls back on the linear μ – Σ relation. The resulting scatter around the corrected μ – Σ relation is 25% at the HSB end and about 50% at the LSB end. The intrinsic scatter in the μ – Σ relation is estimated to be 10%–20%. Thus, if $\mu_{K,0}$ is known, the stellar surface mass density is known to within 10%–20% (random error). Assuming disks have an exponential vertical distribution of mass, the average Υ_*^K is $0.24 M_\odot/L_\odot$, with an intrinsic scatter around the mean of at most $0.05 M_\odot/L_\odot$. This value for Υ_*^K is 20% smaller than we found in Martinsson et al., mainly due to the correction for dark matter applied here. This small scatter means that among the galaxies in our sample, variations in scale height, vertical density profile shape, and/or the ratio of vertical over radial velocity dispersion must be small.

Key words: galaxies: fundamental parameters – galaxies: kinematics and dynamics – galaxies: spiral

1. INTRODUCTION

Mass modeling of rotation curves provided the first qualitative indication that low surface brightness (LSB) disks were submaximal and had lower densities (e.g., de Blok & McGaugh 1997). This method, however, is limited by the disk–halo degeneracy (van Albada et al. 1985), whereby contributions from the disk and halo can range from halo-only to a maximum disk. Measurements of the vertical stellar dispersion of disk galaxies provide a powerful tool to measure the disk surface mass densities (Bahcall 1984), breaking this degeneracy. Results based on vertical stellar velocity dispersion measurements show that even normal surface brightness disks are significantly submaximal (Bottema 1993; Kregel et al. 2005; Bershady et al. 2011; Martinsson et al. 2013b, hereafter DMS-VII), similar to values found from other work, such as planetary nebulae kinematics (Herrmann & Ciardullo 2009) and gravitational lensing (Dutton et al. 2011); work based on hydrodynamical modeling yields higher values (Weiner et al. 2001; Kranz et al. 2003). Results for the Milky Way range from submaximal to maximal depending on the value of the derived radial scale length (e.g., Sackett 1997; Bovy & Rix 2013).

For a self-gravitating disk in equilibrium, the dynamical local surface mass density Σ_{dyn} can be determined from

$$\Sigma_{\text{dyn}} = I\Upsilon_{\text{dyn}} = \sigma_z^2 / (\pi G k h_z), \quad (1)$$

where σ_z is the stellar vertical velocity dispersion, k is a constant depending on the vertical mass distribution (1.5 for an exponential distribution, 2 for an isothermal), h_z is the vertical scale height, I is the surface luminosity density, and Υ_{dyn} is the dynamical mass-to-light ratio of the disk. Thus, to determine the surface mass density (Σ) in a galactic disk, both the vertical distribution of stars and the vertical stellar

velocity dispersion are needed (e.g., Bahcall 1984). To measure the vertical stellar velocity dispersion without the uncertainties introduced by projection effects, face-on galaxies are needed and to measure the vertical distribution of stars unambiguously, edge-on galaxies are needed. It is therefore not possible to measure both simultaneously in external galaxies.

Fortunately, the relation between scale height and scale length is statistically well known from edge-on galaxies (see Bershady et al. 2010b, hereafter DMS-II). Combining this knowledge about scale heights from edge-on galaxies with the measured vertical stellar velocity dispersion from nearly face-on galaxies, one can calculate Σ_{dyn} .

The DiskMass Survey (Bershady et al. 2010a, hereafter DMS-I) has been designed to reliably measure surface brightness, inclination, and vertical velocity dispersion simultaneously (DMS-II; Martinsson et al. 2013a, hereafter DMS-VI). With these measurements, Martinsson et al. (2013b) derived dynamical and stellar surface mass densities as well as the stellar mass-to-light ratio Υ_*^K . Mass modeling based on these Υ_*^K shows disks to be significantly submaximal, with the disks contributing on average $57\% \pm 7\%$ of the rotation velocity at 2.2 disk scale lengths.

In this Letter, we present the correlation between the central extrapolated surface brightness $\mu_{K,0}$ and the surface mass density derived from Equation (1) based on the central extrapolated vertical velocity dispersion $\sigma_{z,0}$, suggesting Equation (1) not only applies locally within individual disks but also describes the properties of disks across different galaxies.

2. SAMPLE AND DATA REDUCTION

The complete DiskMass sample and its selection is described in detail in DMS-I. Here, we use the sample from DMS-VI, consisting of 30 galaxies for which PPAK integral-field

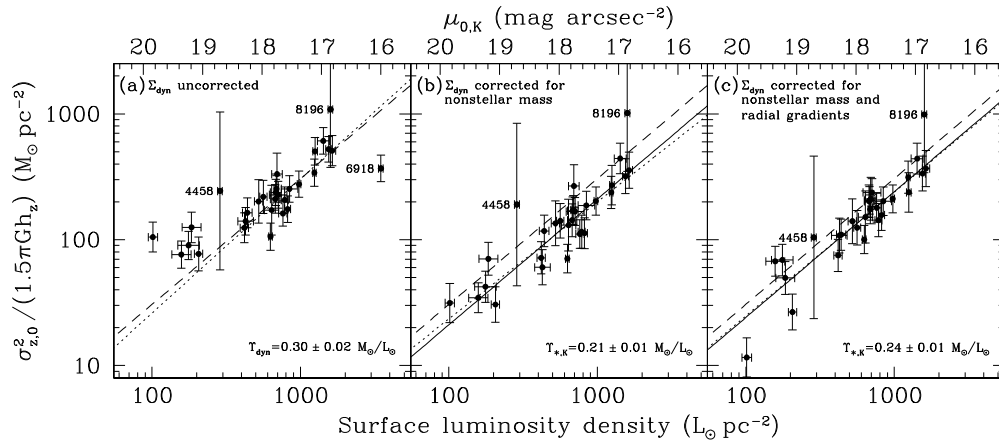


Figure 1. μ - Σ relation is the relation of surface mass density, derived with Equation (1), to surface luminosity density, converted from the K -band surface brightnesses assuming $M_{\odot,K} = 3.30$. Panel (a) shows the μ - Σ relation for the dynamical disk surface mass density Σ_{dyn} . In panel (b), Σ_{dyn} is corrected for the contribution of gas and dark matter to the disk, and in panel (c), Σ_{dyn} is also corrected for the effects of radial gradients in Y_{*}^K . The long-dashed line in panel (a) and solid lines are fits with a slope fixed to -0.4 ; the dotted lines have a free slope. The long-dashed lines in panels (b) and (c) give the μ - Σ relation from panel (a) for reference.

spectroscopic observations are available. The galaxies in this sample span a range in properties (see DMS-VI): Hubble types from Sa to Im (but 83% have Hubble types of Sbc, Sc, or Scd), absolute magnitudes in broadband K_s (hereafter K) from $M_K = -25.5$ to $M_K = -21$, $B - K$ colors from 2.7 to 4.2 mag, and K -band central disk surface brightnesses from 16 to 20 mag arcsec $^{-2}$.

We use the observed line-of-sight velocity dispersions derived as described in DMS-VI. To derive the vertical component of the velocity dispersion σ_z , we follow the same procedure as presented in DMS-VI. For this, we need to assume a triaxial shape of the stellar velocity dispersion ellipsoid (SVE). We assume $\alpha = \sigma_z/\sigma_R = 0.6 \pm 0.15$ and $\beta = \sigma_\theta/\sigma_R = 0.7 \pm 0.04$, following DMS-II. This correction for the SVE shape is done for each measurement of σ_{LOS} in the fibers individually. An exponential function is then fit to all the derived σ_z points, excluding radii affected by the bulge (see DMS-VII). From this fit, we obtain $\sigma_{z,0}$ and $h_{\sigma,z}$, the dispersion scale length, and their uncertainties.

We determined h_z for the galaxies in our sample from their h_R (from DMS-VI), using the relation for the oblateness parameter $q = h_R/h_z$ presented in DMS-II, which we estimated to have an uncertainty of about 25%.

3. RESULTS

Assuming there are no radial gradients in α , β , k , h_z , and Y_{dyn} , Equation (1) can be rewritten in terms of $\sigma_{z,0}$ and $\mu_{K,0}$:

$$\log \Sigma_{\text{dyn},0} = \log (\sigma_{z,0}^2 / (1.5\pi G h_z)) = -0.4\mu_{K,0} + \log Y_{\text{dyn}}^K. \quad (2)$$

Note that $\sigma_{z,0}$ and $\mu_{K,0}$ are not measured in the center, but have been derived from radial fits to the entire disks (excluding parts affected by bulges) and are therefore representative of the entire disk. Unless otherwise specified, we assume $k = 1.5$ (i.e., an exponential distribution).

3.1. The Dynamical Mass-to-light Ratio

In Figure 1(a), the extrapolated central surface brightness $\mu_{K,0}$ is plotted against the extrapolated central surface mass density $\Sigma_{\text{dyn},0}$. Most of the points on this μ - Σ relation form a well-defined correlation, but with an unexpectedly small scatter,

given that α , β , Y_{dyn}^K , k , and q could be different from galaxy to galaxy. There are, however, some outliers. UGC 4458 and UGC 8196 are early-type galaxies with large bulges, leaving only a few points in the σ_z profile that appear unaffected by the bulge, making our derived $\sigma_{z,0}$ uncertain. UGC 6918 is a very high surface brightness (HSB) galaxy that is much more luminous than expected from the Tully-Fisher relation. Finally, all galaxies at the LSB end, labeled in Figure 1(a) with open circles, fall above the correlation outlined by the brighter galaxies.

Focusing on the remaining 22 galaxies for the moment, we find a slope in the μ - Σ relation of -0.43 ± 0.05 (dotted line in Figure 1(a)). This is statistically indistinguishable from the -0.4 slope expected for a linear correlation between the surface mass density and the surface luminosity density. We therefore adopt a slope of -0.4 and fit again (dashed line). Assuming $M_{\odot,K} = 3.30$ (following Westfall et al. 2011; hereafter DMS-IV), we find that the average Y_{dyn}^K is $0.30 \pm 0.02 M_{\odot}/L_{\odot}$. The scatter about the μ - Σ relation is 0.11 ± 0.02 dex.

In DMS-VII, we found $\langle Y_{\text{dyn}}^K \rangle = 0.39 M_{\odot}/L_{\odot}$. The difference between that result and the one presented above is mainly due to the eight galaxies excluded here. Including all galaxies, we find $\langle Y_{\text{dyn}}^K \rangle = 0.40 M_{\odot}/L_{\odot}$, in excellent agreement with our earlier result.

3.2. The Stellar Mass-to-light Ratio

To derive Y_{*}^K from Y_{dyn}^K , we need to correct for the contribution of nonstellar mass in the disk. Both $\mu_{K,0}$ and $\sigma_{z,0}$ were derived from a fit over a large range of the exponential disk. To determine the contribution of the gas, we used a similar method, fitting an exponential to the gas distribution between 0.5 and 3 disk scale lengths and extrapolating that to the center. For UGC 6918, already excluded, this correction is larger than Σ_{dyn} , which we attribute to uncertainties in the derived molecular gas mass (see DMS-VII). After correcting for the contribution of the gas, we find $\langle Y_{*}^K \rangle = 0.26 \pm 0.02 M_{\odot}/L_{\odot}$, and the scatter is 0.12 ± 0.02 dex.

As mentioned above, the galaxies at the LSB end tend to fall above the μ - Σ relation even after correction for the contribution of the gas. LSB galaxies are dominated by dark matter for plausible values of Y_{*} (e.g., Swaters et al. 2003; Kuzio de Naray et al. 2008). The effect of the dark halo on the stellar dynamics

could therefore be non-negligible, as we calculated at the HSB end for UGC 463 (DMS-IV), and larger at the LSB end. To estimate the effect of the dark matter on our results, we used previous work by Bottema (1993). In his Figure 15, Bottema shows the correction to $\sigma_{z,0}$ that is due to the dark matter, as a function of ε , the ratio of dark to stellar density in the midplane. We calculate $\rho_{\text{DM}}(r, z=0)$ from the best fit pseudo-isothermal halo model from DMS-VII. The midplane density for the disk is calculated assuming an exponential vertical density distribution and Υ_{dyn}^K derived above. Within each galaxy, the value of ε is roughly constant between one and three disk scale lengths (see also Figure 17 in DMS-IV); we use the ratio at two disk scale lengths because it is representative of the radial range over which we fit σ_z and μ_K . Among galaxies, ε ranges from 0.15 for galaxies at the HSB end to about 1 at the LSB end. With this ratio and Bottema's curve, we corrected the values of $\sigma_{z,0}$ for the effect of the dark halo.

After $\sigma_{z,0}$ is corrected for both the contribution of gas and dark matter, the LSB galaxies follow the same correlation (see Figure 1(b)). Left free in the fit, the slope is -0.37 ± 0.03 (dotted line). Fixing the slope to -0.4 (solid line), we find that $\langle \Upsilon_*^K \rangle$, now including the LSB end, is $0.21 \pm 0.01 M_\odot/L_\odot$.

The scatter about the correlation has increased to 0.13 ± 0.02 dex, due to the uncertainties associated with the corrections for gas and especially the dark matter. For example, the mass models in DMS-VII used individual Υ_*^K for each galaxy, whereas here we use an average value, but this effect is small because the dark matter dominates. In addition, we should have iterated the mass modeling because changing Υ_*^K will change the halo parameters, which in turn, change Υ_*^K . Tests on individual galaxies indicate this may lower Υ_*^K another 30%. We will revisit the issue of the influence of the dark halo on the disk in a forthcoming paper.

Even though the correction for the contribution of dark matter is uncertain, it is clear that the correction is larger for galaxies with lower surface brightness. With the above method, the correction at the HSB end is about 10% and at the LSB end it is about 50%.

3.3. The Impact of Radial Gradients

Above, we assumed that there are no radial variations in α , β , k , q , and Υ_{dyn} within each galaxy. If there are no gradients, then from Equation (1) it follows that $h_{\sigma,z} = 2h_R$. In DMS-VI, we found that the ratio $\log(h_{\sigma,z}/2h_R) = 0.07 \pm 0.09$, indicating that there is no significant deviation from this expectation on average. However, there is some scatter, suggesting that in some galaxies, radial gradients may be present.

Within galaxies, variations in β with radius are not expected to have much impact due to the near-face-on nature of our sample and the small expected range in β (e.g., DMS-II). Within galaxies, there is little or no radial variation in h_z , at least for late-type galaxies (e.g., de Grijs & Peletier 1997; Bizyaev & Mitronova 2002). Simulations suggest that α is also relatively constant with radius within the disks of late-type disk galaxies (e.g., Minchev et al. 2012). Radial variations within galaxies are therefore likely dominated by variations in Υ_*^K and k . Variations in k could be caused by changes in the relative contributions of stars, gas, and dark matter.

If we assume that radial gradients are dominated by changes in Υ_{dyn} and that both the surface brightness profile and the σ_z profile have an exponential decline, then the effect of a radial gradient can easily be estimated. In that case, from Equation (1),

we find that

$$\Upsilon_{\text{dyn}}(R) = \Upsilon_{\text{dyn},0} e^{(r/h_R)(2-H)/H}, \quad (3)$$

where $H = h_{\sigma,z}/h_R$. For $H = 2$, $\Upsilon_{\text{dyn}}(R)$ is constant with radius, as expected. For other values of H , this is not the case, but there will be some radius r_a for which $\Upsilon_{\text{dyn}}(r_a)$ is representative of the average Υ_{dyn} across the measured range. This radius r_a is different from galaxy to galaxy, but on average $r_a = 1.0h$. With Equation (3) for $r = 1.0h$, we find that the correction factor is $e^{(2-H)/H}$.

Applying this correction converts $\Upsilon_{\text{dyn},0}$ to $\langle \Upsilon_{\text{dyn}}(R) \rangle$, which reduces the scatter in the μ - Σ relation, as shown in Figure 1(c). Left free in the fit, the slope is -0.39 ± 0.03 (dotted line). Fixing the slope to -0.4 (solid line), we find $\langle \Upsilon_*^K \rangle = 0.24 \pm 0.01 M_\odot/L_\odot$. The overall scatter remains 0.13 ± 0.02 dex. At the LSB end the scatter is higher (0.2 dex), likely because $h_{\sigma,z}$ cannot be measured as accurately at the LSB end. In addition, for the LSB galaxies, the contribution of dark matter at large radii increases, which can change the effective k . However, this effect is already corrected for in the dark matter correction above, meaning that the LSB galaxies may be overcorrected. Considering the same 22 galaxies as above, the scatter is reduced to 0.09 ± 0.02 dex, smaller than for the uncorrected μ - Σ relation.

3.4. Intrinsic Scatter

There are three main sources of scatter on the μ - Σ relation. One source is the uncertainties on the adopted parameters α , β , and q . Our adopted scatter of 0.15 in α between galaxies introduces a scatter of 0.11 dex on the μ - Σ relation and the 25% uncertainty on q from galaxy to galaxy also introduces a scatter of 0.11 dex. However, variations in q may be coupled with variations in α because, at a given Υ_{dyn} , galaxies with larger h_z will have higher σ_z as well. Such a coupling, the details of which depend on the in-plane heating of σ_R , would lessen the impact of variations in α and q on the scatter on the μ - Σ relation. Due to the orientation of the galaxy disks, the impact of uncertainties in β and inclination are small.

The second source is the measurement uncertainties on σ_{LOS} , $\mu_{K,0}$, and h_R . These uncertainties contribute 0.05 dex to the scatter.

The remaining source is the intrinsic scatter in the μ - Σ relation (σ_i), mainly due to variations in Υ_* and possibly in k . To estimate σ_i , we compared the measured scatter in the μ - Σ relation to the median uncertainty on Σ_{dyn} . For HSB galaxies, after correction for the contribution of gas, dark matter, and radial gradients, the median uncertainty is 0.12 dex. This is similar to but somewhat higher than the measured scatter of 0.09 dex (about 25%), which could be due to the correlation between α and q mentioned above. Assuming that the measured scatter is dominated by uncertainties in α and q , σ_i must be small, at most about half the measured scatter, i.e., 12%, because otherwise the measured scatter about the μ - Σ relation would have been larger. If we assume instead that α and q do not contribute to the uncertainty on Σ_{dyn} , σ_i is 20%.

4. DISCUSSION AND CONCLUSIONS

Our main result is that $\mu_{K,0}$, the extrapolated central disk surface brightness, and $\Sigma_{\text{dyn},0}$, the extrapolated central disk surface mass density, are tightly correlated for the galaxies in our sample. With the μ - Σ relation, the dynamical surface mass density can be predicted from the surface brightness with an accuracy of about 30% for galaxies brighter than $\mu_{K,0} = 18.5 \text{ mag arcsec}^{-2}$,

but galaxies at the LSB end fall above this μ - Σ relation. After correcting $\Sigma_{\text{dyn},0}$ for the contribution of gas, dark matter, and the effects of radial gradients, the galaxies at the LSB end move onto the μ - Σ relation as well. At the LSB end, the scatter about the μ - Σ relation remains larger than at the HSB end, but at the HSB end the scatter is reduced to about 25%.

The small scatter around the μ - Σ relation is unexpected, given that many of the galaxies' properties may contribute to it, in particular, the parameters α , k , q , and Υ_*^K . Different galaxies may have different star formation histories, which are expected to modulate Υ_*^K . Variations in vertical profile shapes (e.g., due to superthin disks; see Schechtman-Rook & Bershady 2013) may lead to variations in k among galaxies. Dominant disk-heating processes may be different between galaxies, leading to different α . Any of these variations would have increased the scatter in the μ - Σ relation. Given the small scatter in the μ - Σ relation, the variations in these properties among galaxies must be small. Larger variations in these parameters are possible, but only if there is fine-tuning among the parameters (specifically, $\alpha^2 q / (k \Upsilon_*^K)$ should be constant) to maintain the small scatter in the μ - Σ relation.

If we assume conservatively that α and q correlate, as described above, σ_i is about 20% and is dominated by variations between galaxies in k and Υ_*^K . If α and q do not correlate, variations in k and Υ_*^K may be as low as 12%.

Assuming $k = 1.5$ for all galaxies, a slope of -0.4 in the μ - Σ relation, and adopting an intrinsic scatter of 12%, we find that the average $\Upsilon_{\text{dyn}}^K = 0.30 \pm 0.02 M_\odot/L_\odot$, with an intrinsic scatter of $0.04 M_\odot/L_\odot$. If k varies between galaxies, the range in Υ_{dyn}^K may be larger, as long as the product of k and Υ_{dyn}^K remains constant (see Equation (1)). After correction for gas and dark matter, as well as gradients within each galaxy's disk, we find the average $\Upsilon_*^K = 0.24 \pm 0.01 M_\odot/L_\odot$, with an intrinsic scatter of $0.03 M_\odot/L_\odot$. This result suggests that, despite spanning a wide range in properties, galaxies in our sample have a similar Υ_*^K , with only small variations from galaxy to galaxy, as was also found in DMS-VII.

We compare our dynamically inferred Υ_*^K to two canonical stellar population synthesis models with known differences in the treatment late phases of stellar evolution (Bruzual & Charlot 2003, BC03; Maraston 2005, M05). All models predict a range of Υ_*^K depending on age, star formation, and chemical enrichment history. For the restricted subset of models with solar metallicities and exponentially declining star formation rates with e -folding times between 0.1 Gyr and ∞ and ages above 7 Gyr, both models yield similar ranges of $0.4 < \Upsilon_*^K < 0.65$ for the mean color of $g - i = 0.88$ of our sample. For younger ages, mimicking galaxies with more vigorous recent star formation, Υ_*^K drops to 0.25 (0.33) at 3–7 Gyr and 0.15 (0.26) at 0.8–3 Gyr for M05 (BC03), respectively.

Our mean Υ_*^K is compatible with the lower end of the Υ_*^K values predicted by BC03 and M05 for rather young ages (suggesting significant recent star formation). Alternatively, our derived Υ_*^K would change systematically for different adopted values for α , q , or k , while the scatter in the μ - Σ relation would remain the same. To realize $\Upsilon_*^K \sim 0.4$, for example, changes of around 20% are needed in each of α , q , and k . Different adopted initial stellar mass functions would also modulate Υ_*^K (e.g., Conroy et al. 2009).

We note that our sample is biased toward late-type spiral galaxies. The two early-type galaxies in our sample fall above the μ - Σ relation, but are consistent with it within their large

uncertainties on $\sigma_{z,0}$. To verify whether this could play a role, we investigated the results by Herrmann & Ciardullo (2009) and Gerssen & Shapiro Griffin (2012). We cannot make direct comparisons because the analyses were done differently, but we do find that the Sc galaxy in their sample falls on our μ - Σ relation, and the earlier types fall significantly above, consistent with what we find here. This could in part be due to different q ; in DMS-II we found q may be about 50% lower in early-type disk galaxies. However, this can at best explain a small fraction of the difference. To explain the offset, Υ_*^K would have to increase by a factor of two or three toward early-type galaxies. This suggests that the μ - Σ relation presented here could be a slice through a plane in which the Hubble type or a physical property strongly correlated with the Hubble type is a second parameter.

For the sample presented here, the scatter in the μ - Σ relation is small, with an observed scatter at the HSB end of about 25% and an intrinsic scatter of at most 10%–20%. This means that it is possible to determine the stellar surface mass density from the observed surface brightness with an accuracy of 10%–20%. It also means that α , q , and k cannot vary significantly within our sample. Finally, unless k changes from galaxy to galaxy, the small scatter also means that Υ_*^K does not vary more than 10%–20% between the galaxies in our sample and that the average Υ_*^K of the galaxies in our sample is $0.24 M_\odot/L_\odot$, with an estimated intrinsic scatter of at most $0.05 M_\odot/L_\odot$.

M.A.B. acknowledges support from NSF/AST-1009471. T.P.K.M. acknowledges support from The Netherlands Research School for Astronomy (NOVA). K.B.W. acknowledges grants OISE-754437 (NSF) and 614.000.807 (NWO).

REFERENCES

- Bahcall, J. N. 1984, *ApJ*, 276, 156
- Bershady, M. A., Martinsson, T. P. K., Verheijen, M. A. W., et al. 2011, *ApJL*, 739, L47
- Bershady, M. A., Verheijen, M. A. W., Swaters, R. A., et al. 2010a, *ApJ*, 716, 198 (DMS-I)
- Bershady, M. A., Verheijen, M. A. W., Westfall, K. B., et al. 2010b, *ApJ*, 716, 234 (DMS-II)
- Bizyaev, D., & Mitronova, S. 2002, *A&A*, 389, 795
- Bottema, R. 1993, *A&A*, 275, 16
- Bovy, J., & Rix, H.-W. 2013, *ApJ*, 779, 115
- Bruzual, G., & Charlot, S. 2003, *MNRAS*, 344, 1000 (BC03)
- Conroy, C., Gunn, J. E., & White, M. 2009, *ApJ*, 699, 486
- de Blok, W. J. G., & McGaugh, S. S. 1997, *MNRAS*, 290, 533
- de Grijs, R., & Peletier, R. F. 1997, *A&A*, 320, L21
- Dutton, A. A., Brewer, B. J., Marshall, P. J., et al. 2011, *MNRAS*, 417, 1621
- Gerssen, J., & Shapiro Griffin, K. 2012, *MNRAS*, 423, 2726
- Herrmann, K. A., & Ciardullo, R. 2009, *ApJ*, 705, 1686
- Kranz, T., Slyz, A., & Rix, H.-W. 2003, *ApJ*, 586, 143
- Kregel, M., van der Kruit, P. C., & Freeman, K. C. 2005, *MNRAS*, 358, 503
- Kuzio de Naray, R., McGaugh, S. S., & de Blok, W. J. G. 2008, *ApJ*, 676, 920
- Maraston, C. 2005, *MNRAS*, 362, 799 (M05)
- Martinsson, T. P. K., Verheijen, M. A. W., Westfall, K. B., et al. 2013a, *A&A*, 557, A130 (DMS-VI)
- Martinsson, T. P. K., Verheijen, M. A. W., Westfall, K. B., et al. 2013b, *A&A*, 557, A131 (DMS-VII)
- Minchev, I., Famaey, B., Quillen, A. C., et al. 2012, *A&A*, 548, A126
- Sackett, P. D. 1997, *ApJ*, 483, 103
- Schechtman-Rook, A., & Bershady, M. A. 2013, *ApJ*, 773, 45
- Swaters, R. A., Madore, B. F., van den Bosch, F. C., & Balcells, M. 2003, *ApJ*, 583, 732
- van Albada, T. S., Bahcall, J. N., Begeman, K., & Sancisi, R. 1985, *ApJ*, 295, 305
- Weiner, B. J., Sellwood, J. A., & Williams, T. B. 2001, *ApJ*, 546, 931
- Westfall, K. B., Bershady, M. A., Verheijen, M. A. W., et al. 2011, *ApJ*, 742, 18 (DMS-IV)